American Mineralogist, Volume 61, pages 971–978, 1976

The superstructure of meteoritic low tridymite solved by computer simulation

WAYNE A. DOLLASE

Geology Department, University of California
Los Angeles, California 90024

AND WERNER H. BAUR

Department of Geological Sciences
University of Illinois, Chicago, Illinois 60680

Abstract

Below 107°C meteoritic tridymite transforms reversibly to the low-tridymite structure, a superstructure with a cell volume six times the volume of the orthorhombic high-tridymite cell. Low tridymite is monoclinic, space group Cc, with cell dimensions: $a=18.524(4)$, $b=5.0032(15)$, $c=23.810(8)$Å, $\beta=105.82(2)°$. The crystal structure has been determined through computer modeling and refined using 1260 Mo$K\alpha$ reflections ($R=0.069$). The asymmetric unit contains 12 Si atoms and 24 O atoms. The SiO_4 tetrahedra are regular within the margin of error (mean Si–O: 1.601Å). Twenty-three of the 24 Si–O–Si angles fall in the range 142° to 159°, while one is linear (178.5°). The characteristic six-membered rings of the ideal tridymite structure are distorted into two different configurations: two-thirds have a ditrigonal shape (similar to the shape of the rings found in micas and in stuffed derivative structures of tridymite) while one-third have an oval shape (similar to those found in the low-cristobalite structure).

Introduction

In spite of its simple chemical formula, SiO_2 is structurally a remarkably complex material. At least ten polymorphs have been recognized, but the crystal structures of several of these are unknown or only incompletely known. One of the unknown SiO_2 structures is that of meteoritic low tridymite. Tridymite is the stable phase of SiO_2 at low pressure and temperatures between 867 and 1470°C (Boyd and England, 1960). Its stability field is rapidly reduced with increasing pressure. The atomic arrangement has not been studied with modern methods at equilibrium conditions, but it is thought to be closely similar to the ideal hexagonal high-tridymite structure (Gibbs, 1926). Due to the reconstructive nature of transformations to other polymorphs, tridymite tends to persist metastably upon rapid cooling. The crystal structure at 220° has been determined using a sample from the Steinbach meteorite (Dollase, 1967). This structure is orthorhombic, $C222_1$, with an atomic arrangement slightly distorted from the ideal hexagonal structure. Below about 107°C this tridymite undergoes a reversible displacive transformation to the low-tridymite structure. The structural relaxation occurring at the transformation results in the formation of a superstructure with a cell volume six times the volume of the orthorhombic cell.

The meteoritic low tridymite is different from terrestrial low tridymite, which has the diffraction aspect $F***$, orthorhombic (Gardner and Appleman, 1974). The structure of one such terrestrial tridymite has been solved by Konnert and Appleman (1975) in a triclinic $F1$ cell.

To date no systematic method has been presented for the solution of superstructures, although many different techniques have been applied with varying degrees of success. Most of the methods employed the diffraction evidence itself, although this presents a problem, as superstructures are characterized by a small set of intense substructure peaks (containing primarily information on the average structure) and a larger set of much weaker superstructure reflections which contain information about the deviations between the various sub-cells comprising the true cell.

Phase determination and Fourier methods are usually hampered by the paucity and low intensity of the data.

A new development in the solution of superstructures has been the recognition (Meier and Villiger, 1969; Gramlich and Meier, 1971; Baur, 1971, 1972) that the number of near neighbor interatomic distances exceeds the number of positional variables in a structure. Therefore, if the interatomic distances for a particular arrangement can be predicted, then the atomic positions can be adjusted by a least-squares procedure which optimizes the fit between predicted and calculated distances. A recent successful application of this technique has been the solution of the $3\times3\times3$ superstructure of cubic SiP_2O_7 with 50 atoms in the asymmetric unit (Tillmanns *et al.*, 1973). This computer simulation technique has been applied here to the superstructure of low tridymite.

Symmetry of the crystal and collection of intensity data

The tridymite considered here occurs naturally in several meteorites (Dollase and Buerger, 1966), in lunar basalts (Dollase *et al.*, 1971; Appleman *et al.*, 1971), and synthetically in fired ceramic silica brick (Fleming and Lynton, 1960; Dollase and Buerger, 1966) and from sodium tungstate melts (Hoffmann, 1967). In all these cases the tridymite has been characterized by its unit cell and space group symmetry as shown by single-crystal X-ray diffraction methods.

A sample of tridymite from the Steinbach meteorite was kindly provided from the Harvard Museum Collection by Professor Clifford Frondel. An X-ray powder pattern, optical properties, specific gravity, and wet chemical analysis of this material have been reported by Grant (1967). His analysis lists an SiO_2 content of 99.5 weight percent, while the remainder consists of small amounts of Al, Na, and H_2O. About two dozen grains were X-rayed and found to be twinned. The true unit cell and space group were determined by extracting from the composite pattern the set of reflections due to one individual. The systematic absences are $h+k=2n$ (for hkl) and $l=2n$ (for $h0l$), therefore the space group is either Cc or $C2/c$.

The twin individuals are related by the operation of a six-fold twin axis about the pseudohexagonal $[20\bar{1}]$ direction. The effect of the twinning is to superpose exactly reflections of the type $h+l=3n$. All others are separately measurable. Two data sets were collected on two different twinned crystals. A first preliminary set of 760 F_{obs} was measured on an equi-inclination Weissenberg geometry, single-crystal diffractometer (Cu$K\alpha$ with Ni-filter, maximum $\sin\theta/\lambda=0.5\text{Å}^{-1}$). The crystal had twin components comprising 75, 16, 6, 2, 1, and 0 percent of the total grain volume as estimated from the intensities of equivalent, nonoverlapped reflections. From the measurement of composite intensities and knowledge of the individual volumes of different twins, sets of simultaneous equations have been solved, and the reflection intensities due to an untwinned crystal could be obtained.

Although this data set was sufficient to refine the structure described below, it was insufficient to produce acceptably low positional standard errors. Consequently a second, larger data set was collected. For this a crystal was chosen which showed only two of the possible six twin components (with volumes of 71 and 29% of the total grain). The relative volumes were originally determined from the intensities of nonsuperposed reflections and later confirmed in the refinement procedure. Intensity measurements were made on a computer controlled four-circle diffractometer. Mo$K\alpha$ radiation (graphite monochromator) was employed, and all 3351 reflections up to $\sin\theta/\lambda=0.7\text{A}^{-1}$ were measured. A θ–2Θ scan at 2° per minute over a range of one degree above and below the $K\alpha_1$–$K\alpha_2$ doublet was used. Backgrounds were measured on both sides of the scan for a period equal to the peak scan time. However, due to the weak intensities especially of the superstructure reflections, only 1260 total reflections were found to be observable using the criterion that $I>2\sigma(I)$ (where $\sigma(I)$ is the estimated standard error in the intensity calculated from counting statistics). The data were corrected for Lorentz and polarization factors and for twinning but not for absorption ($\mu=8.4\text{cm}^{-1}$). The cell dimensions were determined by least-squares fitting of 15 superstructure reflection positions measured on the diffractometer: $a=18.524(4)$, $b=5.0032(15)$, $c=23.810(8)$Å, $\beta=105.82(2)°$. The calculated density for a composition of $Si_{48}O_{96}$ per unit cell is 2.255 g cm^{-3} as compared with a value of 2.254(5) g cm^{-3} measured by Grant (1967) on the same material.

Solution of the structure

The superstructure was solved by a combination of optimum interatomic distance modeling and least-squares refinement. Computer simulation models with symmetry Cc and $C2/c$ were obtained, starting from the coordinates of the ideal hexagonal high-tridymite structure referred to the monoclinic low-temperature cell. The variable positional parameters in space group Cc or $C2/c$ were then allowed to vary in order to produce a model structure with optimum

Si–O distances (chosen as 1.61Å) and O–O distances appropriate for regular tetrahedra (2.63Å). The Si–O distances were given weights of 1.0, and the O–O distances were assigned weights of 0.5. Si–Si separations were not included, thus optimization of Si–O–Si angles was not part of the modeling process.

In space group *Cc* (noncentric) tridymite has 36 atoms in the asymmetric unit (12 Si atoms and 24 O atoms). The *x* and *z* coordinates of one atom must be kept constant to define the origin, therefore 106 positional parameters had to be determined. In the centrosymmetric group (*C*2/*c*) three oxygen atoms are constrained to lie on symmetry centers, and a fourth oxygen atom is located on a two-fold axis, giving an asymmetric unit of twenty atoms for a total of 49 variable positional parameters. The least-squares optimization procedure, using the program DLS (Meier and Villiger, 1969) converged to an acceptable solution in both centrosymmetric and noncentrosymmetric cases, albeit slowly. In the *Cc* model the final Si–O distances ranged from 1.603 to 1.617Å while tetrahedral O–O edge lengths fell within the range 2.61 to 2.65Å (corresponding to O–Si–O angles of 108.9 to 110.5°). The Si–O–Si angles in the resulting model ranged from 137 to 175°, but were clustered mainly in the interval between 140 and 152°.

For the *C*2/*c* model, Si–O distances fell into the range 1.600 to 1.611Å, tetrahedral edge lengths ran from 2.50 to 2.66Å (corresponding to angles of 102.6 to 112.5°). The Si–O–Si angles ranged from 137 to 180°, the latter value being for the oxygen atoms located at symmetry centers. Two of these centrosymmetrically positioned oxygen atoms (at ¼ ¼ ½ and ¼ ¾ ½) form the edge of a tetrahedron around a silicon atom. Because of the shortness of *b* (=5.0032Å) they are separated by only 2.50Å (resulting in an angle O–Si–O of 102.5°). This is an unlikely feature of the centric model and possibly could be one of the reasons why low tridymite crystallizes in *Cc*. The noncentric model shows distances and angles in slightly better accord with what is thought to be the optimum. This is related to the fact that the noncentric model has twice as many adjustable parameters.

The simulated models were then tested for correctness by comparison of observed X-ray structure factors with the F_{calc} for each model. The noncentric model (based on the preliminary reflection set) yielded an *R*-factor of about 40 percent and was reduced by further refinement to 15 percent. Convergence was slow due to the high parameter correlation coefficients resulting from pseudosymmetry. When individual isotropic temperature factors were allowed to vary, two of them increased to values larger than 40Å^2, indicating that these positions are not occupied by atoms. The computer simulation was repeated for these two atoms, while all other atoms were constrained to their X-ray positions. Continued least-squares refinement based on the X-ray data confirmed the correctness of the new locations of these two atoms by yielding suitable temperature factors. The refinement converged to an *R*-factor of 8 percent for the preliminary data set. A Fourier map showed no significant anomalies. The standard errors in the positional parameters furnished by this data set were, however, unacceptably high, leading to apparent Si–O distances ranging from 1.42 to 1.72Å. The reasons for these large errors may be sought in the lower quality of the preliminary data set, the small $\sin\theta/\lambda$ range of the set, the low intensities of the superstructure reflections, and the pseudosymmetry of the structure. An attempt to refine the centric model with this data set was unsuccessful; the *R*-factor did not drop below 26 percent.

At this point it appeared that the refined noncentric model was basically correct but inaccurate in detail due to the data. Therefore, the second data set was collected and used in the continued least-squares refinement of the *Cc* structure. Using weights determined from counting statistics, the new set converged to a weighted *R*-factor of 0.069 (with individual isotropic temperature factors). A final difference-Fourier map showed densities as large as 0.5e/Å at locations suggesting marked anisotropic thermal motion of the oxygen atoms. Refinement with anisotropic temperature factors was not attempted due to the prohibitive number of least-squares variables necessary for such a model. A table of observed and final calculated structure factors for the noncentric model is available.[1]

The final refined positional and thermal parameters of the structure are given in Table 1 along with their estimated standard deviations. Positional parameter uncertainty was reduced with the second set of data to about 0.01Å for silicon atoms and about 0.02Å for oxygen atoms. A significant reduction of these values would require collection of new data, preferably using a larger crystal in order to increase the ratio of observed to total reflections.

[1] To obtain a copy of the structure factor table, order Document AM-76-023 by remitting $1.00 in advance for the microfiche, payable to the Mineralogical Society of America, 1909 K Street, N.W. Washington, D.C. 20006.

TABLE 1. Final refined positional and thermal parameters of meteoritic low tridymite in space group *Cc*

Atom	x	y	z	B(Å^2)
Si(1)	0.5507(5)	0.541(2)	0.5642(4)	0.9(1)
Si(2)	.7036(5)	.947(2)	.7374(4)	1.2(1)
Si(3)	.4198(5)	.549(2)	.6225(4)	0.7(1)
Si(4)	.5751(5)	.043(2)	.7955(4)	1.1(1)
Si(5)	.9247(5)	.548(2)	.6971(4)	0.8(1)
Si(6)	.7643(5)	.944(2)	.5386(4)	0.9(1)
Si(7)	.8023(5)	.449(2)	.7661(4)	0.8(1)
Si(8)	.6453(5)	.041(2)	.6027(4)	0.7(1)
Si(9)	.8531(5)	.463(2)	.9016(4)	1.0(1)
Si(10)	.9493(4)	.966(2)	.9358(3)	1.0(1)
Si(11)	.7244(5)	.559(2)	.9605(4)	0.9(1)
Si(12)	.5697(5)	.549(2)	.8702(4)	1.1(1)
O(1)	.5749(10)	.351(3)	.8182(8)	1.2(3)
O(2)	.5707(10)	.840(4)	.8476(8)	1.5(3)
O(3)	.7315(10)	.138(4)	.4851(8)	1.8(4)
O(4)	.7509(10)	.644(3)	.5152(8)	1.7(4)
O(5)	.4155(12)	.352(4)	.6741(9)	2.9(5)
O(6)	.4127(10)	.852(4)	.6434(8)	1.9(4)
O(7)	.8773(11)	.164(4)	.9213(8)	1.8(4)
O(8)	.9160(11)	.668(4)	.9361(9)	2.4(4)
O(9)	.7741(10)	.145(4)	.7538(7)	1.8(4)
O(10)	.7336(11)	.643(4)	.7402(8)	2.2(4)
O(11)	.6195(9)	.341(3)	.5847(7)	1.2(3)
O(12)	.5811(10)	.843(3)	.5661(8)	1.9(3)
O(13)	.4966(12)	.511(3)	.6062(9)	2.7(5)
O(14)	.3533(10)	.489(2)	.5665(8)	1.0(4)
O(15)	.6498(12)	.005(4)	.6711(9)	1.8(4)
O(16)	.6524(10)	.996(4)	.7805(8)	2.0(4)
O(17)	.8636(11)	.499(3)	.7328(9)	1.8(4)
O(18)	.8361(13)	.503(3)	.8333(11)	2.6(4)
O(19)	.5052(10)	.993(3)	.7398(7)	1.8(4)
O(20)	.6369(13)	.511(4)	.9268(10)	2.9(5)
O(21)	.9927(12)	.992(2)	.8868(9)	1.4(5)
O(22)	.5 *	.468(4)	.5 *	2.2(3)
O(23)	.7252(12)	.991(3)	.5898(10)	2.3(4)
O(24)	.7744(11)	.521(3)	.9155(9)	1.5(4)

* These parameters were not varied in order to define the origin.

Description and discussion of the crystal structure of low tridymite

Ideal high tridymite (Gibbs, 1926) crystallizes in $P6_3/mmc$. Orthorhombic meteoritic high tridymite (Dollase, 1967) crystallizes in $C222_1$ which is a subgroup of $P6_3/mmc$. Monoclinic meteoritic low tridymite crystallizes in space group *Cc* which is not a subgroup of $C222_1$ (but of course it is a subgroup of $P6_3/mmc$). The supergroup of lowest symmetry (minimal supergroup) common to *Cc* and $C222_1$ is $C\frac{2}{c}\frac{2}{m}\frac{2_1}{m}$ (see unpublished tables of Neubüser and Wondratschek, 1970). It is conceivable that the transformation proceeds through an unstable transitional state of $C\frac{2}{c}\frac{2}{m}\frac{2_1}{m}$ symmetry.

The view along the short *b*-axis (Fig. 1) emphasizes chains of SiO_4 tetrahedra running parallel to the pseudo-hexagonal axis, $[20\bar{1}]$. An analogous view of ideal hexagonal high tridymite would show these tetrahedra in a nontipped position, *ie.* with an O–O edge parallel in projection to the hexagonal axis, and with a tetrahedral face perpendicular to this axis. The relaxation of the structure during the high-low transformation thus involves a complex pattern of tilting tetrahedra. Because the tetrahedra form a corner-sharing (tectosilicate) network, relaxation (*i.e.* rotational and translational reorientation) of an individual tetrahedron requires a cooperative reorientation of the four neighboring tetrahedra with which it shares corners. The connection of these tetrahedra into closed rings (the smallest rings are six-membered) requires that the rings undergo cooperative changes in their geometries. The planar six-membered rings of the ideal high-tridymite structure are oriented perpendicular to the hexagonal axis and form perfect hexagons. In orthorhombic high tridymite at 220°C they remain as nearly perfect hexagons, but successive layers of these rings are slightly offset from a perfect, eclipsed configuration (Dollase, 1967). In the low-tridymite cell the plane of six-membered rings is $(10\bar{1})$ (Fig. 2). The quasiplanar six-membered rings are distorted forming two different geometries: four of the six rings are ditrigonal while the remaining two are of an oval configuration. Each layer of the low-tridymite structure is formed of the same sequence of one oval and two ditrigonal rings. Because the ditrigonal (*D*) rings can be oriented to point along either the positive or negative end of the *b* axis and the oval (*O*) rings can similarly have either of the two orientations displayed in Figure 2, the detailed sequence of rings in any one layer is . . . *O D D O' D' D'* . . . where the primes refer to the alternate orientation.

To complete the tectosilicate framework, the layers of six-membered rings are stacked one on top of another. In the tridymite structure family, six-membered rings stack directly over six-membered rings thus forming continuous channels parallel to the pseudohexagonal axis. In the low-tridymite structure, with the rings relaxed into two different configurations, it is observed that ditrigonal rings may stack above ditrigonal rings or above oval rings and *vice-versa*. That means stacking sequences involving repetition of the same ring type as well as changes of ring type do occur. The repeat period along the pseudohexagonal axis corresponds to 12 layers. The stacking sequence along *any* channel is . . . *O' O D' D D' D O*

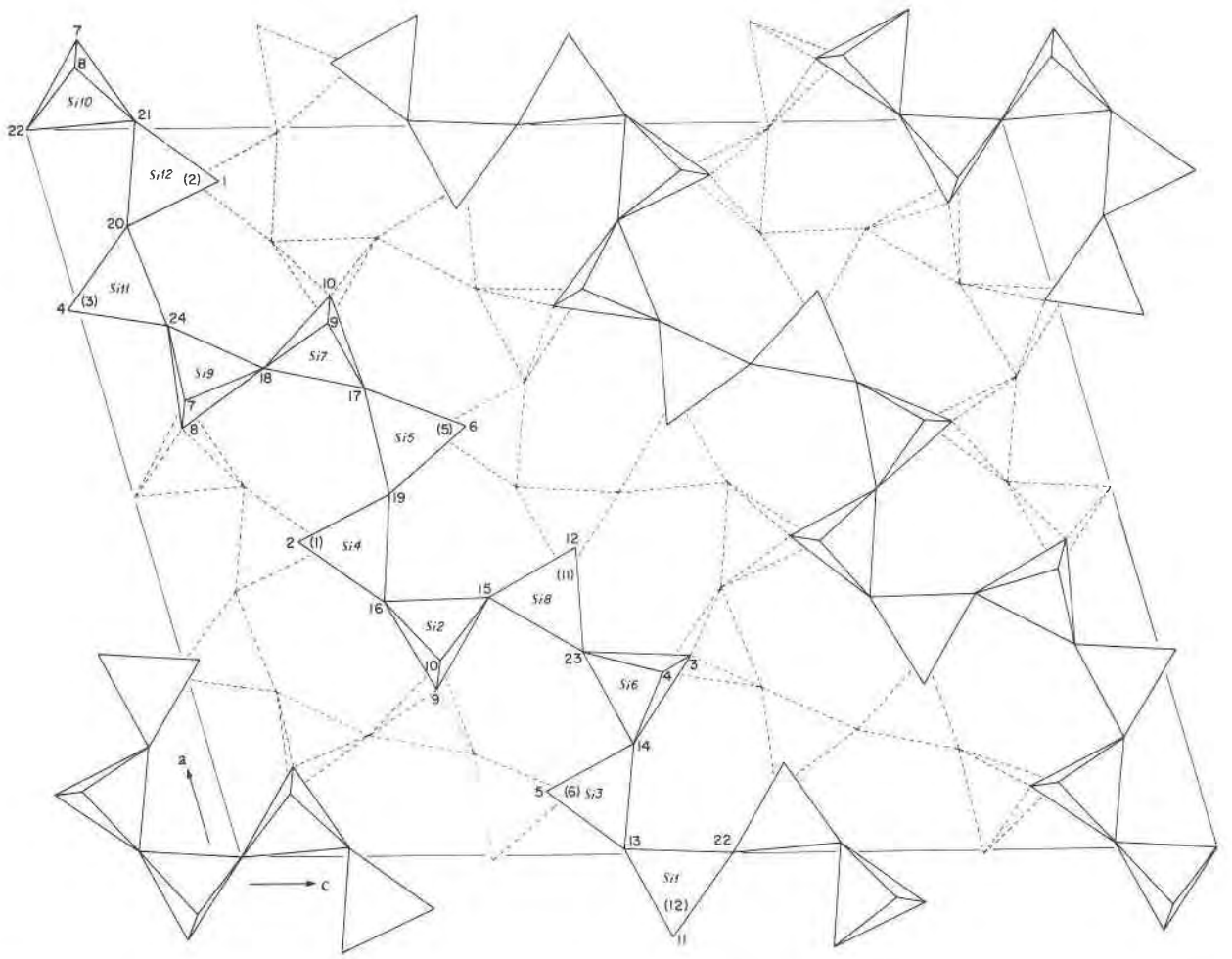

FIG. 1. Projection of the meteoritic low-tridymite structure along the monoclinic *b* axis. The numbers placed at tetrahedral corners identify the oxygen atoms.

O' D D' D D' . . . The entire sequence of ring types as projected along *b* is diagrammatically represented in Figure 3. This figure also outlines the pseudohexagonal supercell, the true monoclinic supercell, and the (high) subcell.

Only certain combinations of adjoining rings are possible: in Figure 2 it can be seen that forming a row of (say) *D*-type rings along the *b* axis also forms the left half of the next row of rings in the [101] direction, forcing this adjoining row to be either *D*-type or *O'*-type, but not allowing *D'* or *O*-type rows of rings. Such restrictions in connectivity have the effect of inducing a longer-range positional correlation in the structure (longer range refers to neighbors other than next neighbors). Therefore it might be expected that just above the transformation temperature when the perfect long-range ordering of the low structure is lost but the rings are probably still distorted, that some degree of local and/or temporal positional correlation might still exist. The marked diffraction effects (existence of temperature-dependent, sharp satellite reflections) observed just above the transformation temperature (Dollase, 1966) are taken as evidence of such imperfect longer-range positional correlation.

In tridymite derivative structures and in low cristobalite, topologically identical layers of six-membered rings also show the two types of ring configuration. Generally, however, individual structures display only one type of ring. In kalsilite, $KAlSiO_4$ (Perrotta and Smith, 1965), which is representative of a large family of stuffed tetrahedral framework structures, the rings are observed to be all ditrigonal. Low cristobalite at room temperature (Dollase, 1965) shows planes of oval-configuration six-membered rings. Wright and Leadbetter (1975) have proposed a short-

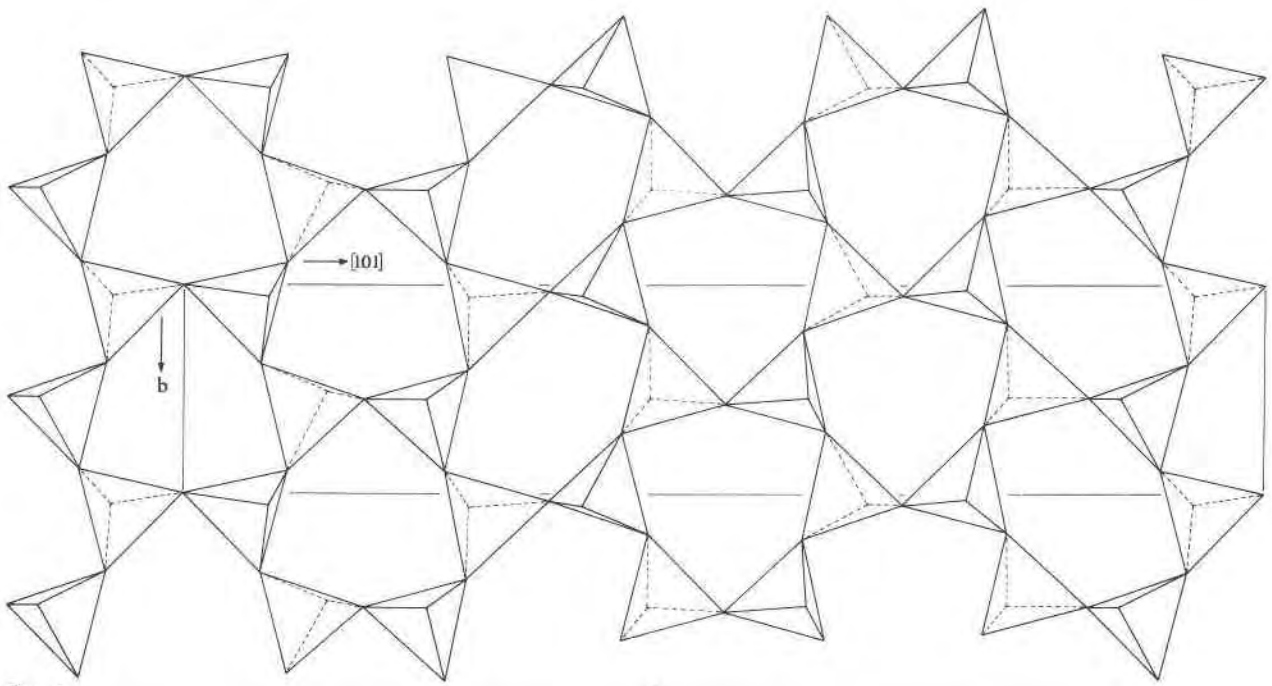

FIG. 2. Projection of a slab of the low-tridymite structure onto (10$\bar{1}$) showing the two types of six-membered ring configurations—ditrigonal and oval.

range ordered model for cristobablite *above* its transformation from low cristobablite in space group $I\bar{4}2d$. Examination of their proposed model shows that the six-membered rings are present in an all-ditrigonal configuration, suggesting that the transformation involves a change from one type of ring distortion to the other.

The 48 independent Si–O bond lengths (Table 2) average to 1.601Å. The twelve independent SiO_4 tetrahedra have mean bond lengths ranging from 1.59 to 1.62Å. Considering a probable standard error in the bond lengths of about 0.02Å, the range of individual Si–O distances (1.55 to 1.65Å) amounts to 2 ½ sigma on either side of the average. The distribution of individual bond lengths around their mean is approximately gaussian. The O–Si–O angles have values within 5° of the ideal tetrahedral angle. The O–O tetrahedral edge lengths range from 2.52 to 2.68Å. Of the 24 independent Si–O–Si angles, all but one fall within the interval of 142 to 159°. The remaining angle is very nearly linear (178.5°). The average of all Si–O–Si angles is 149.8°. The result of the refinement of the isotropic thermal parameters is consistent with the low coordination number and low density of this phase. Silicon atom temperature factors run from 0.7 to 1.2Å^2 (average 0.90) and those of oxygen range from 1.0 to 2.9Å^2 (average 1.94).

Success of the computer simulation model

Comparison of the final refined positional parameters of the *Cc* model with those of the original noncentric computer simulation model shows large discrepancies involving Si atoms of as much as 0.6Å and oxygen atom positions differing by up to 1.5Å. However, the starting model was so close to the X-ray model that 34 of the 36 atoms *did* refine to their correct locations without intervention in the refinement process, and the remaining two atoms could be correctly placed in a second cycle of simulation. In terms of the types and distributions of the six-membered rings, the simulated noncentric model was entirely composed of oval rings, thus in this respect a low-cristobalite analog. In terms of atomic positions, the difference between the starting model and the refined structure was due to the y coordinates of four pairs of atoms (two Si atom pairs and two O atom pairs). The correct structure can be obtained from the simulation model by interchange of the y coordinates of these pairs of atoms. Schematically this means that where the model "zigged," it should have "zagged." Conceivably, the modeling procedure could have been improved by inclusion of optimum Si–O–Si angles, but the observed spread in these angles suggests that this factor is of limited significance.

Although the structure of low tridymite is definitely noncentrosymmetric, as shown by the lack of success in refining a centric model below $R = 23$ percent with either data set, there is a strong component of pseudocentrosymmetry in the final X-ray structure. The centrosymmetric optimum distance model has remarkable similarities to the refined *Cc* structure. The arrangement of ring types is the same. The x and z coordinates of all the atoms as refined in *Cc* lie within 0.02 of the fractional coordinates of the *C*2/*c* simulation model. Thus in projection, the low-tridymite structure is very nearly centric. The differences in the refined *Cc* and simulated *C*2/*c* structures are caused by differences in the y coordinates of corresponding atoms (amounting to as much as 1.4Å). Those cases where the atom in *C*2/*c* is constrained to lie on a symmetry element, but the corresponding atom in *Cc* is not so constrained, display the largest deviations between the two structures. The Si–O–Si angles constrained to be 180° in the *C*2/*c* model refine to values between 147 and 155° in the correct structure. Oxygen O(17), the atom showing a nearly linear Si–O–Si angle in the *Cc* model, does not correspond to one of these symmetry-constrained atoms.

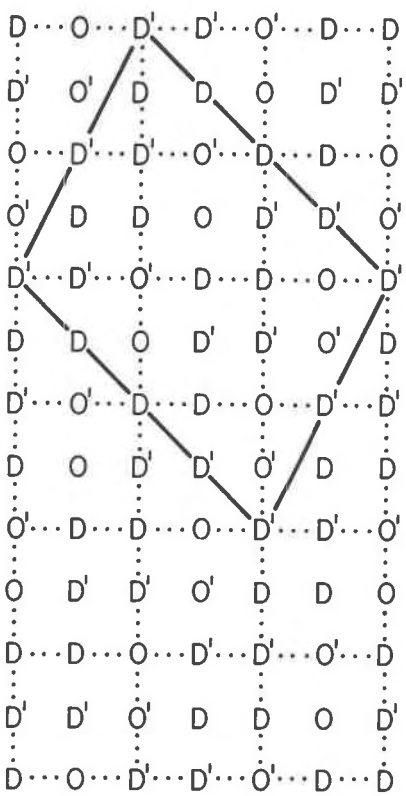

FIG. 3. Representation of the sequence of six-membered ring types in low tridymite as viewed along the *b* axis. The entire array outlines the pseudohexagonal supercell, the solid lines show the true, monoclinic cell, and the dotted lines show the high-tridymite subcell.

TABLE 2. Interatomic distances and angles in meteoritic low tridymite

Si–O distances (e.s.d.=0.02Å)

Si(1)-O(11)	1.59Å	Si(5)-O(6)	1.58Å	Si(9) -O(18)	1.58Å
Si(1)-O(22)	1.60	Si(5)-O(19)	1.58	Si(9) -O(7)	1.60
Si(1)-O(13)	1.60	Si(5)-O(17)	1.61	Si(9) -O(8)	1.60
Si(1)-O(12)	1.61	Si(5)-O(5)	1.61	Si(9) -O(24)	1.61
mean*	1.601	mean	1.595	mean	1.597
Si(2)-O(16)	1.60	Si(6)-O(3)	1.59	Si(10)-O(21)	1.59
Si(2)-O(9)	1.60	Si(6)-O(23)	1.60	Si(10)-O(22)	1.60
Si(2)-O(10)	1.61	Si(6)-O(4)	1.60	Si(10)-O(8)	1.61
Si(2)-O(15)	1.65	Si(6)-O(14)	1.62	Si(10)-O(7)	1.62
mean	1.612	mean	1.599	mean	1.606
Si(3)-O(14)	1.58	Si(7)-O(17)	1.57	Si(11)-O(24)	1.61
Si(3)-O(13)	1.59	Si(7)-O(18)	1.57	Si(11)-O(3)	1.62
Si(3)-O(5)	1.59	Si(7)-O(10)	1.59	Si(11)-O(20)	1.62
Si(3)-O(6)	1.61	Si(7)-O(9)	1.60	Si(11)-O(4)	1.62
mean	1.592	mean	1.587	mean	1.616
Si(4)-O(16)	1.59	Si(8)-O(11)	1.60	Si(12)-O(2)	1.55
Si(4)-O(19)	1.60	Si(8)-O(12)	1.61	Si(12)-O(20)	1.58
Si(4)-O(2)	1.62	Si(8)-O(23)	1.61	Si(12)-O(21)	1.61
Si(4)-O(1)	1.63	Si(8)-O(15)	1.62	Si(12)-O(1)	1.61
mean	1.611	mean	1.609	mean	1.587

Si–O–Si angles (e.s.d.=1.3°)

Si(4)-O(1) -Si(12)	147.3°	Si(1) -O(13)-Si(3)	153.7°
Si(4)-O(2) -Si(12)	149.2	Si(3) -O(14)-Si(6)	148.0
Si(6)-O(3) -Si(11)	147.2	Si(2) -O(15)-Si(8)	146.7
Si(6)-O(4) -Si(11)	148.7	Si(2) -O(16)-Si(4)	154.2
Si(3)-O(5) -Si(5)	145.4	Si(5) -O(17)-Si(7)	178.5
Si(3)-O(6) -Si(5)	146.0	Si(7) -O(18)-Si(9)	159.3
Si(9)-O(7) -Si(10)	141.7	Si(4) -O(19)-Si(5)	155.9
Si(9)-O(8) -Si(10)	144.6	Si(11)-O(20)-Si(12)	148.9
Si(2)-O(9) -Si(7)	146.4	Si(10)-O(21)-Si(12)	148.7
Si(2)-O(10)-Si(7)	145.8	Si(1) -O(22)-Si(10)	154.9
Si(1)-O(11)-Si(8)	146.1	Si(6) -O(23)-Si(8)	143.2
Si(1)-O(12)-Si(8)	142.6	Si(9) -O(24)-Si(11)	151.5

*The means were calculated before the values were rounded.

Acknowledgments

The original data set was measured in the laboratory of Professor M. J. Buerger at MIT. The second data set was collected in the Chemistry Department at UCLA, where Dr. B. T. Huie and Professor C. E. Strouse provided valuable assistance. This study was supported, in part, by the Earth Science Section, National Science Foundation through NSF Grant # DES74-19918. We thank the Computer Center of the University of Illinois, Chicago, for providing computer time and Professor H. Bärnighausen for discussions (see also Bärnighausen, 1975).

References

APPLEMAN, D., H. NISSEN, D. STEWART, J. CLARK, E. DOWTY AND J. HUEBNER (1971) Studies of lunar plagioclase, tridymite and cristobalite. *Proc. 2nd Lunar Sci. Conf.* **1**, 117–133.

BÄRNIGHAUSEN, H. (1975). Group-subgroup relations between space groups as an ordering principle in crystal chemistry: the "family tree" of perovskite-like structures. *Acta Crystallogr.* **A31,** S3.

BAUR, W. H. (1971) Geometric refinement of the crystal structure of β-Mg_2SiO_4. *Nat. Phys. Sci.* **233,** 135–137.

———(1972) Computer simulated crystal structures of observed and hypothetical Mg_2SiO_4 polymorphs of low and high density. *Am. Mineral.* **57,** 709–731.

BOYD, F. R. AND J. L. ENGLAND (1960) The quartz–coesite transition. *J. Geophys. Res.* **65,** 749–756.

DOLLASE, W. A. (1965) Reinvestigation of the structure of low cristobalite. *Z. Kristallogr.* **121,** 369–377.

———(1966) *The crystal structures of some phases of silica.* Ph.D. Thesis, Massachusetts Institute of Technology, Cambridge, Massachusetts.

———(1967) The crystal structure at 220°C of orthorhombic high tridymite from the Steinbach meteorite. *Acta Crystallogr.* **23,** 617–623.

———AND M. J. BUERGER (1966) Crystal structure of some meteoritic tridymites. (Abstr.) *Geol. Soc. Am. Prog. 1966 Annu. Meet.* 54–55.

———, R. A. CLIFF AND G. W. WETHERILL (1971) Note on tridymite in rock 12021. *Proc. 2nd Lunar Sci. Conf.* **1,** 141–142.

FLEMING, J. E. AND F. LYNTON (1960) A preliminary study of the crystal structure of low tridymite. *Phys. Chem. Glasses,* **1,** 148–151.

GARDNER, S. P. AND D. E. APPLEMAN (1974) X-ray crystallography and polytypism of naturally-occurring tridymite, SiO_2. *Am. Crystallogr. Assoc. Program and Abstracts.* **2,** 271.

GIBBS, R. E. (1926) The polymorphism of silicon dioxide and the structure of tridymite. *Proc. R. Soc. London,* **A113,** 351–368.

GRAMLICH, V. AND W. M. MEIER (1971) The crystal structure of hydrated NaA: a detailed refinement of a pseudosymmetric zeolite structure. *Z. Kristallogr.* **133,** 134–149.

GRANT, R. W. (1967) New data on tridymite. *Am. Mineral.* **52,** 536–540.

HOFFMANN, W. (1967) Gitterkonstanten und Raumgruppe von Tridymit bei 20°C. *Naturwiss.* **54,** 114.

KONNERT, J. H. AND D. E. APPLEMAN (1975) Terrestrial low tridymite: refinement of the three dimensional structure. *Geol. Soc. Am. Abstracts with Programs* **7,** 1151.

MEIER, W. M. AND H. VILLIGER (1969) Die Methode der Abstandsverfeinerung zur Bestimmung der Atomkoordinaten idealisierter Gerüststrukturen. *Z. Kristallogr.* **129,** 411–423.

PERROTTA, A. J. AND J. V. SMITH (1965) The crystal structure of kalsilite. *Mineral. Mag.* **35,** 588–595.

TILLMANNS, E., W. GEBERT AND W. H. BAUR (1973) Computer simulation of crystal structures applied to the solution of the superstructure of cubic silicondiphosphate. *J. Solid State Chem.* **7,** 69–84.

WRIGHT, A. F. AND A. J. LEADBETTER (1975) The structure of the beta-cristobalite phases of SiO_2 and $AlPO_4$. *Phil. Mag.* **31,** 1391–1401.

Manuscript received, September 29, 1975; accepted for publication, February 25, 1976.